Journal of
Water & Climate Change

IWA PUBLISHING

Journal of Water and Climate Change Vol 14 No 1, 156 doi: 10.2166/wcc.2022.244

Evaluation of multiple bias correction methods with different satellite rainfall products in the Main Beles Watershed, Upper Blue Nile (Abbay) Basin, Ethiopia

Asmare Belay Nigussie[a,*], Hailu Wondmageghu Tenfie[a], Fasikaw A. Zimale[b], Andualem Endalew[a] and Genet Wudiye[a]

[a] School of Civil and Water Resource Engineering & Architecture, Kombolcha Institute of Technology, Wollo University, Kombolcha 1145, Ethiopia
[b] Faculty of Civil and Water Resources Engineering, Bahir Dar Institute of Technology, Bahir Dar University, Bahir Dar 6000, Ethiopia
*Corresponding author. E-mail: belay1asmare@gmail.com; asmarebelay@kiot.edu.et

ABSTRACT

This study investigates the utility of satellite-based rainfall products and the performance of bias correction methods in one of the sub-basins of the Upper Blue Nile Basin (Main Beles basin). Four satellite rainfall products are used: Climate Prediction Center (CPC) MORPHing technique (CMORPH), Precipitation Estimation from Remotely Sensed Information using Artificial Neural Networks (PERSIANN), Tropical Rainfall Measuring Mission Multi-Satellite Precipitation Analysis (TMPA) 3B42V7 (TMPA 3B42V7), and Climate Forecast System Reanalysis (CFSR). The performance of the satellite rainfall products (SRPs) was compared using three bias correction methods (Delta, Empirical Quantile Mapping (EQM), and Quantile Mapping (QM)) on five metrological stations. Six statistical criteria were used to evaluate these methods on the period 2003–2016 at daily and monthly scales. The results showed that SRPs and bias correction methods of CMORPH_QM ($r = 0.538$) and TMPA_3B42V7_EQM ($r = 0.95$) data showed good performance, while PERSIANN_EQM ($r = 0.348$) and PERSIANN_Delta ($r = 0.83$) performed worst at daily and monthly time scales, respectively. This study assessed the importance of SRPs and bias correction methods to use in data scarce regions for water resources planning and other related sectors.

Key words: Delta, EQM, Main Beles, QM, satellite rainfall products

HIGHLIGHTS

- Four satellite rainfall products (CMORPH, CFSR, PERSIANN and TMPA_3B42V7) and three bias correction methods (i.e., Delta, Quantile Mapping (QM) and Empirical Quantile Mapping (EQM)) were evaluated.
- Only CMORPH using QM and TMPA_3B42V7 using EQM data showed good performance, while PERSIANN using EQM and PERSIANN using Q3 Delta performed worst at daily and monthly time scales, respectively.

GRAPHICAL ABSTRACT

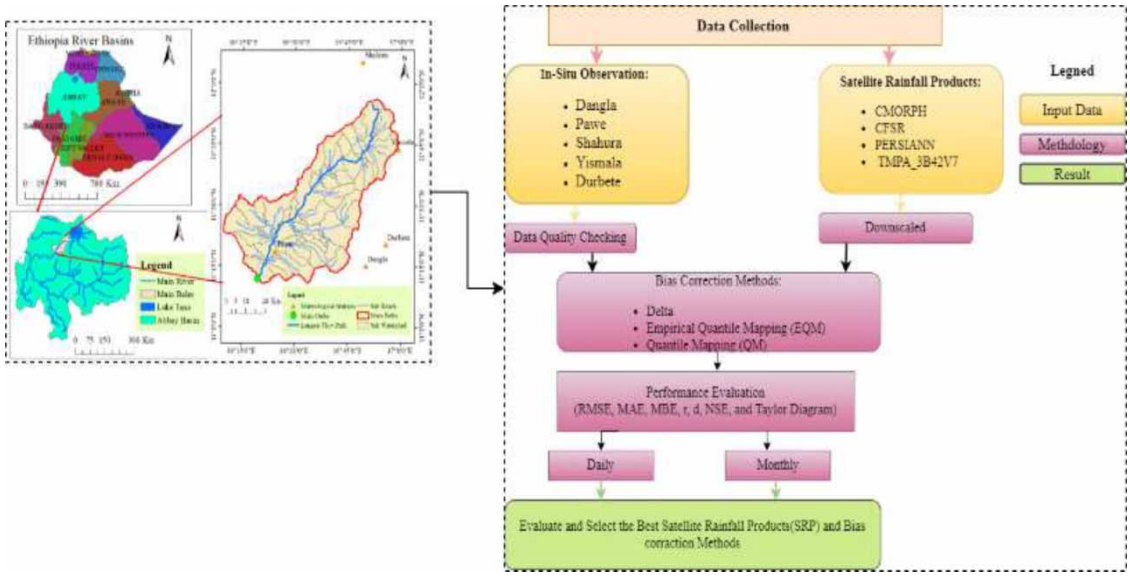

1. INTRODUCTION

In Ethiopia, the assessment of water resource issues is difficult in data-sparse areas because estimating water availability necessitates an understanding of rainfall variability both spatially and temporally (Belay *et al.* 2019). Good-quality precipitation data estimates are critical to the accuracy and dependability of any hydrologic study, whether it is for flood-forecasting, drought-monitoring, water resource management, or climate change effect assessment (Hamlet & Lettenmaier 1999). Rain gauges provide a direct physical measurement of surface precipitation, although they are subject to certain errors due to location, spatial scale (point), wind, and mechanical flaws, among other things (Derin & Yilmaz 2014). This implies that observed rainfall data are better than satellite rainfall estimation, but the lack of sufficient rain gauge observations has an impact on water resource assessment due to the spatial variability of rainfall.

Because precipitation is the most important atmospheric input to land surface hydrology models, accurate precipitation inputs are critical for accurate hydrologic prediction. Ground-based precipitation measurements are sparse or non-existent in many remote parts of the world, particularly in developing countries, due to the high cost of establishing and maintaining infrastructure. Inconsistencies in instrumentation and administrative limitations on data access for rivers that cross international borders further impede the effective use of hydrological models to support reliable flood and drought diagnosis and forecasting (Habib *et al.* 2014; Hall *et al.* 2014; Revilla-Romero *et al.* 2015). Both of these constraints apply to the Main Beles sub-basin of the Upper Blue Nile Basin.

Precipitation estimates based on satellites with high spatial and temporal resolution and wide coverage of the area offer a potential alternative source of impact data for hydrological models in areas where traditional *in situ* precipitation observations are not always available. The increasing availability of high-resolution (and near real-time) satellite-based rainfall estimates has significant potential in applications like hydrological analysis for engineering design, assimilation of precipitation data into forecast models, flood forecasting, and water resource management in general (Liu *et al.* 2012; Zambrano-Bigiarini *et al.* 2017; Moges *et al.* 2022). These applications could have far-reaching implications for various developing countries, such as Ethiopia, which lacks ground-based rain gauges and does not have radar capabilities to measure representative rainfall magnitude. However, there are errors in satellite-based rainfall estimations, which raise a number of scientific concerns. How accurate are satellite-based rainfall products? Is it possible to employ high-resolution satellite rainfall products (SRPs) for hydrological purposes? The hydrological community faces a challenge due to a lack of understanding about the accuracy of those satellite products, particularly in complex terrain and less gauged areas (Funk *et al.* 2015). The fact that rain gauge-based rainfall data are point data that represent an area defined by a limited radius surrounding the device's location is a prominent aspect (Collischonn *et al.* 2008). Furthermore, the density of measuring stations is uneven between areas, and

their positions favor accessible lower-lying places (López López *et al.* 2018). As a result, a high-resolution spatial dataset that can efficiently capture variations in spatial precipitation is required.

For the goal of reanalyzing satellite-derived precipitation data, the Delta, Empirical Quantile Mapping (EQM), and Quantile Mapping (QM) bias correction methods were applied. Furthermore, the Main Beles River basin was selected since it is one of the tributary river basins in the Upper Blue Nile Basin (Yasir *et al.* 2014). The Main Beles River basin encompasses five metrological stations with a range of climates and physical attributes. Accurate precipitation data for the Main Beles River basin will aid in the prediction of extreme occurrences such as floods and droughts.

Therefore, Climate Prediction Center Morphing (CMORPH) (Joyce *et al.* 2004; Haile *et al.* 2013; Yang *et al.* 2021), Climate Forecast System Reanalysis (CFSR) (Bao & Zhang 2013; Dile & Srinivasan 2014), Precipitation Estimation from Remotely Sensed Information using Artificial Neural Networks (PERSIANN) (Nguyen *et al.* 2019), and Tropical Rainfall Measuring Mission (TRMM) Multi-satellite Precipitation Analysis (TMPA_3B42V7) (Prakash *et al.* 2016; Vu *et al.* 2018) SRPs are employed in this study. These SRPs (PERSIANN, CMORPH, TMPA_3B42V7 and CFSR) were selected based on the following criteria: public domain dataset, long-term data availability, reasonable spatiotemporal resolution, near-real-time availability and their wide applicability in Africa (Dinku *et al.* 2007; Thiemig *et al.* 2012; Dembélé & Zwart 2016; Haile *et al.* 2013; Prakash *et al.* 2015).

Some of the previous studies which investigated the Main Beles River Basin involved hydrological responses of a catchment to climate change (Yimer *et al.* 2009; Ebrahim *et al.* 2013; WaleWorqlul *et al.* 2018), hydrological responses to land use/cover changes (Woldesenbet *et al.* 2017), hydropower (Annys *et al.* 2019), Soil erosion (Kebede *et al.* 2021), soil management (Molla *et al.* 2022), assessment of water resource and forecasting (Hamza & Getahun 2022) and spatial and temporal variability in hydrological responses (Lemann *et al.* 2018). It is still a common practice that rainfall is interpolated from point rain gauge measurements in water resources and other related studies. However, such a method is expensive, particularly for developing countries like Ethiopia, because many gauges are needed to capture typically large rainfall variability, so often, gauge numbers are compromised. As such, interpolation can create high bias. Satellite rainfall estimates can fill this gap by providing spatio-temporal data coverage, although processed satellite rainfall products have often substantial biases when compared with true, gauge measurements, mainly due to different spatial resolutions. Besides, the performance of satellite products is different in different areas due to geographical and climatic variations. To fill this gap in a given study area, it is therefore essential to evaluate the error of different satellite rainfall estimates against the rain gauge network of that area, based on that choose an optimal satellite rainfall product for that particular area, and finally remove the bias of the satellite rainfall product.

This research looks at the capability and limitations of SRPs (CMORPH, CFSR, PERSIANN, and TMPA_3B42V7), as well as the performance of three bias correction methods (Delta, EQM, and QM) for the Main Beles basin with five metrological stations like Pawe, Dangla, Shahura, Durbete, and Yismala. By comparing statistical properties and Taylor diagrams (Ayoub *et al.* 2020; Centella-Artola *et al.* 2020), the performance of SRPs and bias correction approaches have been evaluated.

2. DATA AND STUDY AREA

2.1. Study area

The Main Beles catchment is located in the western part of the Upper Blue Nile Basin, Ethiopia. It is one of the tributary river basins of the Upper Blue Nile Basin, Ethiopia. This is situated on the plateau of the north-western highlands of Ethiopia near Lake Tana in a geographic location from a latitude of 10°50′N to 11°50′N and a longitude of 36°10′E to 37°00′E. The topography of the area is mostly flat with altitudes between 999 m and 2,724 m above sea level.

The total area of the watershed is estimated to be 3,424.36 km^2 (Figure 1). It is one of the major sub-basins of the Upper Blue Nile Basin. The mean monthly rainfall of Durbete, Dangla, Pawe, Shahura, and Yismala stations is used for the period of 2003–2016 (Figure 2). The mean annual maximum rainfall recorded at the watershed is 1,837.21 mm, and the annual average daily minimum and maximum temperature ranges between 12 and 38 °C.

2.2. Data

2.2.1. Observed rainfall data

Observed rainfall data are the most demanding input data for daily and monthly comparisons of SRPs and bias correction methods. Therefore, the Ethiopian National Meteorological Agency provided the observed rainfall data. Data were collected from five stations in the Main Beles watershed, including Pawe, Dangla, Shahura, Durbete, and Yismala (Figure 3).

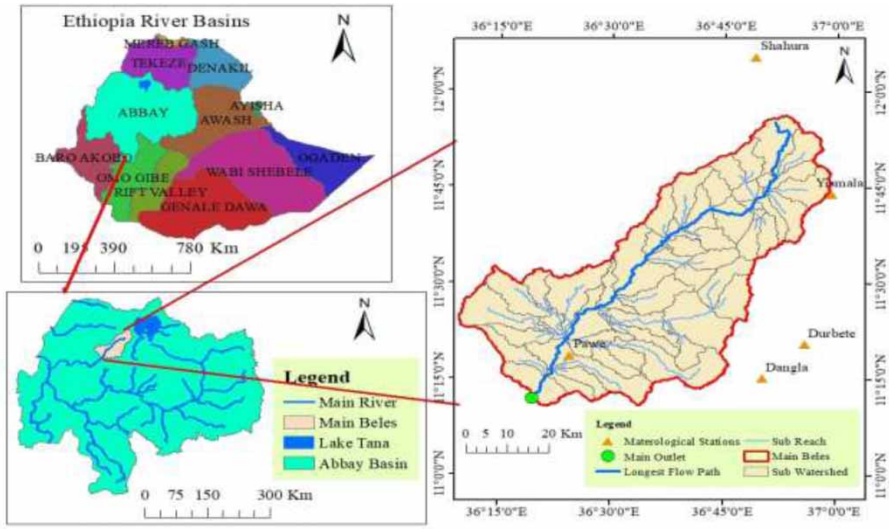

Figure 1 | Geographical location map of the Main Beles River Basin (metrological and hydrological stations). The inset maps show the locations of the Abay basin within Ethiopia and Main Beles within the Abay basin.

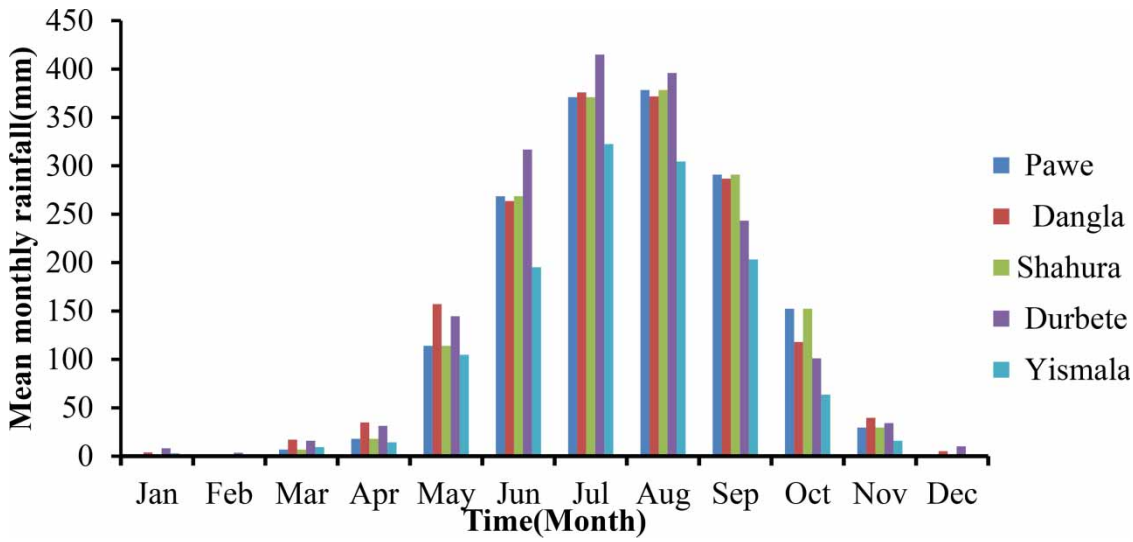

Figure 2 | Mean monthly rainfall distribution of the meteorological stations for the period of 2003–2016.

2.2.2. CMORPH satellite rainfall products

The CMORPHing approach (Climate Prediction Center (CPC) MORPHing technique) generates worldwide precipitation studies with extremely high spatial and temporal resolution. This technique exclusively uses precipitation estimations acquired from low-orbiter satellite microwave observations, whose features are transmitted via spatial propagation information derived purely from geostationary satellite IR data (Joyce *et al.* 2004). Algorithms for the Satellite Program series of special sensor microwave/imagers (SSM/I) (Ferraro 1997), Advanced Microwave Sounding Unit (AMSU-B) (Ferraro *et al.* 2000), and TRMM Microwave Image (TMI) are used to generate these estimates (Kummerow *et al.* 2001). From December 3, 2002 to the present, CMORPH provides daily precipitation products with a grid resolution of 0.07277° latitude/longitude (8 km at the equator), a temporal resolution of 30 min, and a geographical coverage of 60°S–60°N latitude globally (Joyce *et al.* 2004). https://climatedataguide.ucar.edu/ has CMORPH data.

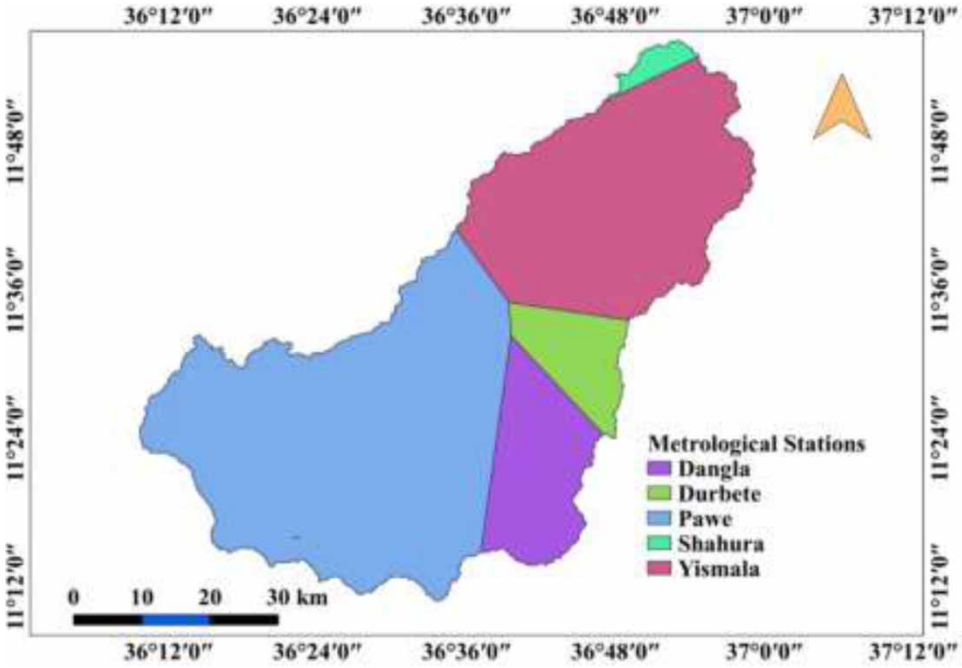

Figure 3 | Thiessen Polygon showing the contribution of meteorological stations in the Main Beles watershed.

2.2.3. TMPA_3B42V7 satellite rainfall products

The TRMM Multi-Satellite Precipitation Analysis (TMPA) product's latest post-real-time data, TMPA 3B42V7, are superior to all prior versions (Yong *et al.* 2014). Since January 1998, the 3B42V7 dataset has covered the global latitude belt from 50°S to 50°N, with a spatial resolution of 0.25° by 0.25° and a temporal resolution of 3 h (Huffman *et al.* 2007). The Goddard Earth Sciences Data and Information Services Center (https://mirador.gsfc.nasa.gov) provides daily precipitation data from 2000 to 2015. The daily 3B42V7 data are consolidated into monthly mean values and include a timeframe of 0:00 UTC–24:00 UTC with the gauge observation.

2.2.4. PERSIANN satellite rainfall products

The Center for Hydrometeorology and Remote Sensing (CHRS) at the University of California, Irvine (UCI) developed the Precipitation Estimation from Remotely Sensed Information using Artificial Neural Networks (PERSIANN) system, which uses neural network function classification/approximation procedures to quantify an estimate of rainfall rate at each $0.25° \times 0.25°$ pixel of the infrared brightness temperature image provided by geostationary satellites (Hsu *et al.* 1997). When independent rainfall estimates are available, an adaptive training feature makes it easier to update the network parameters. The PERSIANN system was originally built on geostationary infrared imagery, but it was later expanded to include both infrared and visible imagery. The PERSIANN algorithm is used to generate global rainfall using the geostationary long-wave infrared imagery (Sorooshian *et al.* 2014). From 2000 to the present, PERSIANN provides daily precipitation products with a spatial resolution of 0.25° 0.25° and a spatial coverage of 60°S–60°N latitude, near real-time with a 2-day delay (Nguyen *et al.* 2018). https://chrsdata.eng.uci.edu/contains PERSIANN data.

2.2.5. CFSR satellite rainfall products

CFSR is a third-generation reanalysis product. It is a global high-resolution system that includes the atmosphere, ocean, land, surface, and sea ice to provide the best assessment of the state of these coupled domains throughout this time period. The CFSR incorporates (1) atmosphere–ocean connection during the creation of the 6-h riddle field, (2) an interactive model of sea ice, and (3) satellite radiation assimilation. The global CFSR atmosphere has a resolution of 38 km (T382) with 64 levels. With 40 levels and data available from 1979-01-01 to 2014-07-31, the global ocean is at 0.25° near the equator, extending to 0.5° beyond the tropics. There are four soil levels in the global land surface model and three levels in the global sea ice

model. The CFSR atmospheric model includes observed CO_2 fluctuations, as well as aerosol and other trace gas and solar variations. The scenario evaluated will include estimations of changes in the climate of the Earth's system as a result of these variables. The current CFSR will be extended in the future as a real-time operating product from the research data archive (RDA) summary on CFSR (Sharp *et al.* 2015; Liu *et al.* 2018; Wei *et al.* 2021). CFSR data are available at https://globalweather.tamu.edu/.

3. METHODS

In this study, four SRPs (CMORPH, CFSR, TMPA3B42V7, and PERSIANN) were investigated to identify the best product to use for the spatial and temporal assessment of any hydrologic study, either related to flood-forecasting, drought-monitoring, water resource management, or climate change impact assessment at daily and monthly time scales. The evaluation was carried out using data for the period from 2003 to 2016 for those SRPs but did not include CFSR SRPs for intercomparison because the variation of availability of rainfall data records from 1979-01-01 to 2014-07-3. Three bias correction approaches were used for the intercomparison of each satellite's product like Delta, EQM, and QM.

3.1. Bias correction methods

There are numerous statistical bias correction methods for precipitation and temperature; the Statistical Downscaling of General Circulation Models (SDGCM) tool is available on the website https://agrimetsoft.com/sd-gcm for downscaling. In this tool, there are three statistical downscaling models: the Delta, the QM and the EQM. The tool is very useful that can carry out the downscaling project for a list of stations in one run and perform both monthly and daily data compared to other tools (Martinez-Villalobos & Neelin 2019). This tool is better to improve the fitting of climate model simulations to observations in the control period, in order to enhance reliability (Boé *et al.* 2007; Oruc 2022).

3.1.1. Delta statistical method

This method was used to derive downscaled weather data, computing the ratio between averaged observation and SRPs data and multiplying this ratio by the satellite rainfall data. It is calculated for precipitation using Equation (1) as follows:

$$P\text{sat}^{\text{Delta}} = P_{\text{sat}} * \frac{\bar{P}_{\text{obs}}}{\bar{P}_{\text{sat}}} \tag{1}$$

where $P\text{sat}^{\text{Delta}}$ is the corrected precipitation data from the satellite-based precipitation data, P_{sat} is the uncorrected precipitation data (or satellite-based data), $\bar{P}_{\text{sat}}$ is the average of the satellite-based precipitation data corresponding monthly (January–December) and daily over the study period, and $\bar{P}_{\text{obs}}$ is the average of the observed precipitation data corresponding monthly and daily over the study period.

3.1.2. EQM statistical method

The EQM method can be applied to any kind of climatic variable. Its principle is based on point-wise daily-constructed empirical cumulative distribution functions (ECDFs). It is distinguished from other distribution mapped-based approaches that focus on precipitation and which only estimate the ECDFs for wet days (Martinez-Villalobos & Neelin 2019; Enayati *et al.* 2021). Its comparative advantage stems from the fact that it can produce possible ECDFs for both dry and wet days. The frequency of precipitation occurrences along with standard deviations can be simultaneously corrected in the EQM approach. The corrected precipitations can, respectively be expressed as follows:

$$P_{\text{sat}}^{\text{EQM}} = \text{ECDF}_{\text{Obs},m}^{-1}(\text{ECDF}_{\text{sat},m}(P_{\text{sat},m,d})) \tag{2}$$

where $P_{\text{sat}}^{\text{EQM}}$ is the corrected precipitation data from the satellite-based precipitation data using EQM methods, $\text{ECDF}_{\text{Obs},m}^{-1}$ is the inverse of empirical cumulative distribution functions of observed precipitation data corresponding monthly and daily over the study period, $\text{ECDF}_{\text{sat},m}$ is empirical cumulative distribution functions of satellite-based precipitation data corresponding monthly and daily over the study period, and $P_{\text{sat},m,d}$ is uncorrected precipitation data (or satellite-based data) corresponding monthly and daily over the study period.

3.1.3. QM statistical method

The original QM method is a non-parametric bias correction BC method generally applicable to all possible distributions of rainfall (Ringard *et al.* 2017; Luo *et al.* 2018).

3.2. Performance metric index of statistical evaluation

In order to evaluate the performance of the gridded precipitation bias correction methods, several statistical indicators were applied to measure the difference between the corrected and observed data by comparing the average pixel-by-pixel difference. Let $(P_{\text{obs1}}, P_{\text{sat1}})$ and $(P_{\text{obs2}}, P_{\text{sat2}}) \ldots (P_{\text{obs } n}, P_{\text{sat } n})$ be n pairs of values from two (observed and bias-corrected precipitation) different datasets. These parameters are calculated as follows:

$$\text{RMSE} = \sqrt{\frac{\sum (P_{\text{obs},j} - P_{\text{sat},j})^2}{n}} \tag{3}$$

$$\text{NSE} = 1 - \frac{\sum_{i=0}^{n} (P_{\text{Obs},i} - P_{\text{Sat},i})^2}{\sum_{i=0}^{n} (P_{\text{Obs},i} - \overline{P_{\text{Obs}}})^2} \tag{4}$$

$$r = \frac{\sum_{i=0}^{n} (P_{\text{Obs},i} - \overline{P_{\text{Obs}}})(P_{\text{Sat},i} - \overline{P_{\text{Sat}}})}{\sqrt{\sum_{i=0}^{n} (P_{\text{Obs},i} - \overline{P_{\text{Obs}}})^2} \sqrt{\sum_{i=0}^{n} (P_{\text{Sat},i} - \overline{P_{\text{Sat}}})^2}} \tag{5}$$

$$\text{MBE} = \frac{1}{n} \sum_{i=0}^{n} (P_{\text{Obs},i} - P_{\text{Sat},i}) \tag{6}$$

$$\text{MAE} = \frac{1}{n} \sum_{i=0}^{n} |P_{\text{Obs},i} - P_{\text{Sat},i}| \tag{7}$$

$$d = 1 - \frac{\sum_{i=0}^{n} (P_{\text{Obs},i} - P_{\text{Sat},i})^2}{\sum_{i=0}^{n} (|P_{\text{Sat},i} - \overline{P_{\text{Obs}}}| + |P_{\text{Obs},i} - \overline{P_{\text{Obs}}}|)}, \quad 0 \le d \le 1 \tag{8}$$

where NSE means the Nash–Sutcliffe Efficiency, RMSE means the root mean square error, r means Pearson's correlation coefficient, MBE means mean bias error, MAE means mean absolute error, d means the index of agreement, $P_{\text{Obs},i}$ means observed precipitation data corresponding monthly and daily over the study period i, $P_{\text{Sat},i}$ means corrected precipitation data (or satellite-based data) corresponding monthly and daily over the study period i, $\overline{P_{\text{Sat}}}$ means the average of the satellite-based precipitation data, $\overline{P_{\text{Obs}}}$ means the average of the observed precipitation data, and n is the number of samples.

3.2.1. Taylor diagram

We apply a Taylor diagram to evaluate differences in datasets generated by respective bias correction schemes by providing a summary of how well bias correction results match gauge rainfall in terms of pattern, variability, and magnitude of the variability. Visual comparison of SRE performance is done by analyzing how well patterns match each other in terms of Pearson's product–moment correlation coefficient (R), root mean square difference (E), and the ratio of variances on a 2D plot (Taylor 2001; Conti *et al.* 2014). The reason that each point in the 2D space of the Taylor diagram can represent the above three different statistics simultaneously is that the centered pattern of root mean square difference (E^i) and the ratio of variances are related by the following equation:

$$E^i = \sqrt{\sigma_f^2 - \sigma_r^2 - 2\sigma f \sigma r R} \tag{9}$$

where σ_f and σ_r are the standard deviation of SRPs and observed rain gauge rainfall, respectively.

Development and applications of Taylor diagrams have roots in climate change studies (Taylor 2001; Smiatek *et al.* 2016) but also have frequent applications in environmental model evaluation studies (Srivastava *et al.* 2015). Bhatti *et al.* (2016) propose the use of Taylor's diagrams for assessing the effectiveness of SRP bias correction schemes. The most effective bias correction schemes will have data that lie near a point marked 'reference' on the *x*-axis, a relatively high correlation coefficient, and a low root mean square difference. Bias correction schemes matching gauge-based standard deviation have patterns that have the right amplitude.

Generally, the overall procedure of the evaluation of the performance of bias correction methods (Delta, EQM, and QM) and SRPs in the Main Beles basin is shown in Figure 4.

4. RESULTS AND DISCUSSION

4.1. Daily and monthly evaluation of bias correction methods

The performance evaluation criteria and the Delta, QM, and EQM methods for refining CMORPH, PERSIANN, TMPA_3B42V7, and CFSR SRPs used in study stations in the Main Beles basin for both daily and monthly rainfall analysis are shown in Tables 1–4. The effectiveness of the bias reduction approaches utilized in this study is determined by the rainfall measuring station and the satellite observation. Based on the overall performance of six performance evaluations, the Delta approach improved the quality of CFRS rainfall in all stations for both daily and monthly time scales. In the case of CMORPH SRP, the Delta method was best among EQM and QM on both daily and monthly time scales for all weather stations (Pawe, Shahura, Dangla, Durbete, and Yismala) except Durbete and Dangla at daily base QM best. For example, for the Dangla station (CMORPH), Delta bias correction evaluation criteria of RMSE (average 9.24 mm day^{-1}) were relatively close to zero, whereas EQM and QM showed higher values (average 10.44 and 9.87 mm day^{-1}), respectively,

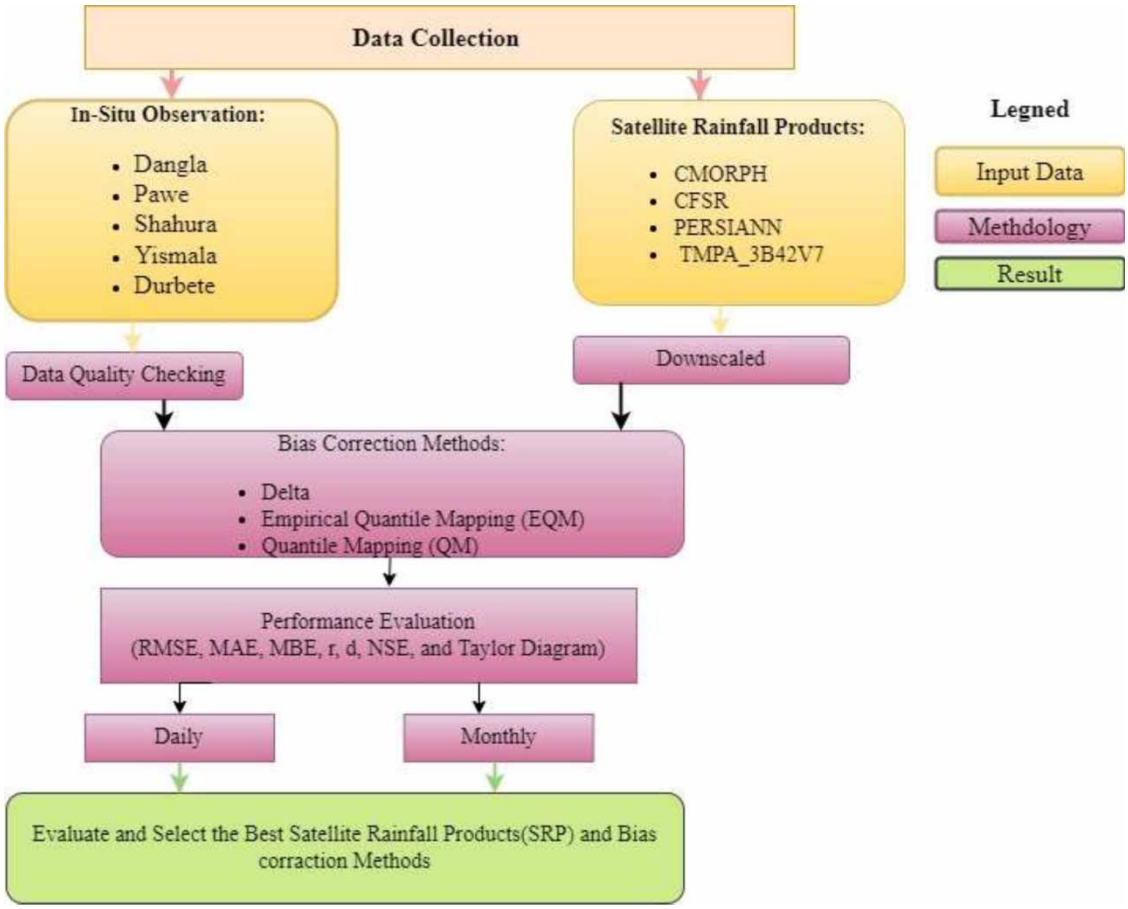

Figure 4 | The flowchart of satellite rainfall validation and merging approach.

Table 1 | Summary of CMORPH bias correction and evaluation of daily and monthly comparisons of Delta, EQM, and QM statistical tools at five observed stations

		Performance evaluation methods											
		Daily						Monthly					
Station	Bias correction	RMSE	*r*	MAE	MBE	*d*	NSE	RMSE	*r*	MAE	MBE	*d*	NSE
Pawe	Delta	**9.24**	0.45	**4.40**	**0.00**	0.65	**0.03**	**2.47**	0.88	**1.48**	**0.00**	**0.94**	**0.77**
	EQM	10.44	0.45	5.13	1.43	0.64	−0.25	3.25	0.88	1.98	1.43	0.91	0.60
	QM	9.87	**0.47**	4.96	1.38	**0.66**	−0.11	3.12	**0.89**	1.89	1.38	0.92	0.63
Dangla	Delta	8.64	0.49	**4.17**	**0.00**	0.69	−0.01	**1.92**	0.93	**1.20**	**0.00**	**0.96**	**0.85**
	EQM	8.85	0.52	4.63	1.33	0.70	−0.06	2.50	**0.94**	1.65	1.33	0.95	0.74
	QM	**8.59**	**0.53**	4.47	1.26	**0.71**	**0.00**	2.41	**0.94**	1.56	1.25	0.95	0.76
Shahura	Delta	**7.54**	0.47	**3.68**	**0.00**	**0.66**	**0.07**	**2.31**	0.87	**1.56**	**0.01**	**0.91**	**0.75**
	EQM	9.65	**0.50**	5.78	3.68	0.65	−0.53	4.66	0.87	3.76	3.67	0.82	−0.04
	QM	9.82	**0.50**	5.71	3.54	0.65	−0.58	4.59	**0.88**	3.63	3.54	0.83	−0.01
Durbete	Delta	8.68	0.50	**4.22**	**0.00**	0.69	−0.04	**2.41**	0.89	**1.44**	**0.00**	**0.94**	**0.78**
	EQM	8.59	0.53	4.43	0.96	0.71	−0.02	2.60	**0.91**	1.74	0.96	**0.94**	0.75
	QM	**8.39**	**0.54**	4.35	0.91	**0.72**	**0.03**	2.55	**0.91**	1.68	0.91	**0.94**	0.76
Yismala	Delta	**7.46**	0.41	**3.50**	**0.00**	0.62	**− 0.18**	**2.01**	0.87	**1.21**	**0.00**	**0.93**	**0.75**
	EQM	7.82	0.46	4.08	1.54	0.65	−0.29	2.79	**0.90**	1.83	1.54	0.91	0.52
	QM	7.70	**0.47**	4.01	1.47	**0.65**	−0.25	2.72	**0.90**	1.75	1.46	0.91	0.54

Bold numbers show the best-performing bias correction approach from the candidates.
Root mean square error (RMSE), correlation coefficient (*r*), MAE, MBE, index of agreement (*d*), and Nash–Sutcliffe Efficiency model are shown. The RMSE, MAE, and MBE values are shown in units of millimeters.

Table 2 | Summary of PERSIANN satellite rainfall bias correction and evaluation daily and monthly comparisons of Delta, EQM, and QM statistical tools at five observed rainfall stations

		Performance evaluation methods											
		Daily						Monthly					
Station	Bias correction	RMSE	*r*	MAE	MBE	*d*	NSE	RMSE	*r*	MAE	MBE	*d*	NSE
Pawe	Delta	**10.13**	**0.36**	**4.88**	**0.00**	**0.58**	**− 0.17**	**2.96**	**0.83**	**1.78**	**0.00**	**0.90**	**0.67**
	EQM	10.85	0.35	5.25	0.43	0.57	−0.35	3.22	0.81	1.95	0.43	**0.90**	0.61
	QM	10.99	0.35	5.21	0.36	0.56	−0.38	3.21	0.81	1.93	0.36	**0.90**	0.61
Dangla	Delta	9.71	0.42	4.63	**0.00**	0.63	−0.27	2.56	0.87	1.57	**0.00**	0.93	0.73
	EQM	**9.04**	**0.44**	4.58	0.04	**0.65**	**− 0.10**	**2.37**	**0.88**	**1.52**	0.04	**0.94**	**0.77**
	QM	9.49	0.42	**4.56**	−0.08	0.63	−0.22	2.50	0.87	1.53	−0.09	0.93	0.74
Shahura	Delta	8.38	0.45	3.73	**0.00**	0.65	−0.15	2.19	0.89	1.27	**0.00**	**0.94**	0.77
	EQM	8.14	0.46	3.74	0.20	**0.66**	−0.09	2.17	0.89	1.29	0.20	**0.94**	**0.78**
	QM	**8.13**	**0.47**	**3.69**	0.11	**0.66**	**− 0.08**	**2.15**	**0.89**	**1.26**	0.10	**0.94**	**0.78**
Durbete	Delta	10.75	0.37	5.09	**0.00**	0.58	−0.59	3.04	0.83	1.86	**− 0.01**	**0.91**	0.65
	EQM	**9.12**	**0.40**	**4.60**	−0.56	**0.62**	**− 0.14**	**2.77**	**0.85**	**1.73**	−0.56	**0.91**	**0.71**
	QM	9.77	0.38	4.71	−0.65	0.60	−0.31	2.93	0.83	1.80	−0.65	0.90	0.68
Yismala	Delta	7.87	0.42	3.56	**0.00**	0.62	−0.31	2.07	0.87	1.28	−0.01	0.93	0.74
	EQM	**7.30**	**0.44**	**3.49**	0.10	**0.65**	**− 0.12**	**1.93**	**0.89**	**1.23**	0.10	**0.94**	**0.77**
	QM	7.50	0.43	3.48	0.00	0.64	−0.19	1.98	0.88	1.23	**0.00**	**0.94**	0.76

Bold numbers show the best-performing bias correction from the candidates.

deviating from zero at daily time step and monthly comparisons of this station. Delta bias correction evaluation criteria of RMSE (average 2.47 mm month^{-1}) were relatively close to zero, whereas EQM and QM showed higher values (25 and 3.12 mm month^{-1}; Table 1).

Table 3 | Summary of TMPA_3B42V7 satellite rainfall bias correction and evaluation daily and monthly comparisons of Delta, EQM, and QM statistical tools at five observed rainfall stations

		Performance evaluation methods											
		Daily						Monthly					
Station	Bias correction	RMSE	*r*	MAE	MBE	*d*	NSE	RMSE	*r*	MAE	MBE	*d*	NSE
Pawe	Delta	**9.58**	**0.45**	**4.53**	**0.00**	**0.65**	**− 0.05**	**2.45**	0.88	**1.51**	**− 0.01**	**0.94**	**0.77**
	EQM	10.01	**0.45**	4.82	0.60	**0.65**	− 0.14	2.64	**0.89**	1.64	0.59	**0.94**	0.74
	QM	10.02	**0.45**	4.78	0.52	**0.65**	− 0.15	2.63	**0.89**	1.60	0.51	**0.94**	0.74
Dangla	Delta	10.66	0.36	5.18	**0.00**	0.57	−0.53	2.05	0.92	1.24	0.00	**0.96**	0.83
	EQM	**9.53**	**0.39**	5.01	0.24	**0.61**	**− 0.23**	**1.84**	**0.93**	1.24	0.24	**0.96**	**0.86**
	QM	9.66	**0.39**	**4.96**	0.10	0.60	−0.26	1.85	0.93	**1.19**	**0.10**	**0.96**	**0.86**
Shahura	Delta	8.37	0.46	**3.79**	**0.00**	0.66	−0.15	**1.70**	0.93	1.14	**0.00**	**0.96**	**0.86**
	EQM	**8.26**	**0.50**	4.11	1.02	**0.68**	**− 0.12**	1.94	**0.94**	1.43	1.02	**0.96**	0.82
	QM	8.43	0.49	4.09	0.91	**0.68**	− 0.16	1.90	0.93	**1.36**	0.91	**0.96**	0.83
Durbete	Delta	9.38	0.49	4.35	**0.00**	0.68	−0.21	1.70	**0.95**	**1.10**	**0.00**	**0.97**	0.89
	EQM	**8.23**	**0.53**	**4.10**	− 0.04	**0.71**	**0.07**	**1.59**	**0.95**	**1.10**	− 0.04	**0.97**	**0.90**
	QM	8.56	0.51	4.12	−0.12	0.70	−0.01	1.62	**0.95**	1.08	−0.12	**0.97**	**0.90**
Yismala	Delta	8.01	0.37	**3.79**	**0.00**	0.59	−0.36	**1.77**	0.90	1.08	**0.00**	**0.95**	**0.81**
	EQM	**7.81**	**0.41**	4.03	0.79	**0.62**	**− 0.29**	1.89	**0.91**	1.27	0.79	**0.95**	0.78
	QM	7.88	**0.41**	4.00	0.69	**0.62**	− 0.31	1.86	**0.91**	**1.21**	0.69	**0.95**	0.79

Bold numbers show the best-performing bias correction from the candidates.
Root mean square error (RMSE), correlation coefficient (*r*), MAE, MBE, index of agreement (*d*), and Nash–Sutcliffe Efficiency (NSE) model are shown. The RMSE, MAE, and MBE values are shown in millimeters.

Table 4 | Summary of CFSR satellite rainfall bias correction of evaluation daily and monthly comparisons using Delta, EQM, and QM statistical tools and five observed rainfall stations

		Performance evaluation methods											
		Daily						Monthly					
Station	Bias correction	RMSE	*r*	MAE	MBE	*d*	NSE	RMSE	*r*	MAE	MBE	*d*	NSE
Pawe	Delta	10.07	**0.40**	**4.84**	**0.00**	0.57	**−0.16**	**4.47**	0.74	**2.48**	− 0.01	**0.84**	**0.31**
	EQM	11.13	0.36	5.50	1.27	0.56	−0.42	5.48	0.75	2.93	1.25	0.81	−0.04
	QM	**10.25**	0.36	5.27	1.29	**0.60**	− 0.20	4.89	**0.79**	2.66	1.27	**0.85**	0.18
Dangla	Delta	**7.92**	0.48	**4.05**	**0.00**	0.67	**0.13**	**2.68**	0.87	**1.66**	**− 0.01**	**0.93**	**0.71**
	EQM	9.64	0.47	5.25	2.28	0.65	−0.29	4.69	0.87	2.82	2.26	0.86	0.11
	QM	8.73	**0.51**	5.01	2.30	**0.69**	− 0.06	4.17	**0.90**	2.62	2.28	0.88	0.30
Shahura	Delta	**7.62**	0.46	**3.53**	**0.00**	0.65	**0.02**	**3.04**	0.83	**1.75**	**0.00**	**0.90**	**0.57**
	EQM	8.60	0.47	4.26	1.60	0.65	−0.25	4.21	0.84	2.13	1.59	0.86	0.17
	QM	7.98	**0.51**	4.10	1.57	**0.69**	− 0.08	3.88	**0.87**	2.06	1.56	0.88	0.29
Durbete	Delta	7.80	0.52	**3.91**	**0.00**	0.70	**0.12**	**2.24**	0.92	**1.41**	**− 0.01**	**0.96**	**0.82**
	EQM	8.56	0.50	4.33	0.80	0.69	−0.06	2.82	0.92	1.74	0.79	0.94	0.71
	QM	**7.75**	**0.55**	4.07	0.83	**0.72**	0.13	2.50	**0.94**	1.58	0.82	0.95	0.77
Yismala	Delta	**7.37**	0.43	**3.52**	**0.00**	0.64	**−0.05**	**2.57**	0.86	**1.50**	**− 0.01**	**0.92**	**0.60**
	EQM	8.13	0.46	4.13	1.44	0.65	−0.28	3.67	0.88	2.01	1.43	0.87	0.19
	QM	7.70	**0.48**	4.00	1.42	**0.67**	− 0.15	3.46	**0.90**	1.93	1.41	0.89	0.28

Bold numbers show the best-performing bias correction from the candidates.
Root mean square error (RMSE), correlation coefficient (*r*), MAE, MBE, index of agreement (*d*), and Nash–Sutcliffe Efficiency (NSE) model are shown. The RMSE, MAE, and MBE values are shown in millimeters.

In the case of PERSIANN SRPs, Delta for Pawe, QM for Dangla & Shahura and EQM for Yismala stations are the best BC approaches on daily and monthly time scales (Table 2). For example, for the Pawe station (PERSIANN), Delta bias correction evaluation criteria of RMSE (average 10.13 mm day^{-1}) were relatively close to zero, whereas EQM and QM showed higher

values (average 10.85 and 10.99 mm day^{-1}, respectively; Table 2). The TMPA 3B42V7 SRP is best for Delta at the Pawe station both daily and monthly, EQM for Dangla, Yismala, and Shahura stations on a daily time scale but Delta on a monthly time scale, and EQM for the Durbete station on both daily and monthly time scales. For example, EQM bias correction evaluation criteria of the correlation coefficient (r) value of 0.51 were relatively close to one, whereas Delta and QM showed higher values (average 0.49 and 0.51, respectively) deviating from one at daily and monthly time step comparisons of this station. The correlation coefficient (r) is demonstrated to have a comparable value in Durbete station, which is 0.95 substantially close to one at the monthly time scale based on Delta, EQM, and QM bias correction. For all weather stations, the CFSR SRP Delta method performed best among EQM and QM on both daily and monthly time scales (Pawe, Shahura, Dangla, Durbete, and Yismala). For example, the Delta bias correction evaluation criterion of correlation coefficient (r) value for the Shahura station (CFSR) was 0.51, relatively close to one, whereas EQM and QM showed higher values (0.47 and 0.46, respectively), deviating from one at daily and monthly time step comparisons of this station (Table 4).

Table 5 shows that the best bias correction evaluation of both daily and monthly time step comparisons using Delta, EQM, and QM statistical methods corresponds with SRPs (CMORPH, TMPA 3B42V7, PERSIANN, and CFSR) and five rainfall gauge stations. Delta bias correction methods outperformed other bias correction methods (EQM and QM) at the Pawe station for all daily and monthly SRPs (CMORPH, TMPA 3B42V7, PERSIANN, and CFSR). For the Dangla station, EQM was chosen for TMPA 3B42V7 and PERSIANN bias correction on a daily and monthly basis, but Delta was chosen for CFSR bias correction on a daily and monthly basis, and QM was chosen for CMORPH SRPs on a daily and monthly basis. Delta for CMORPH and CFSR bias correction methods and QM for PERSIANN bias correction methods were chosen from the Shahura station for both daily and monthly time scales, but EQM at daily and Delta at monthly time scales were chosen for TMPA 3B42V7 satellite rainfall bias correction. For the Durbete station, EQM for TMPA 3B42V7 and PERSIANN bias correction methods and Delta for CFSR bias correction methods were chosen for both daily and monthly time scales but QM at daily and Delta at monthly for CMORPH satellite rainfall bias correction. For the Yismala station, Delta for CMORPH and CFSR bias correction methods and EQM for PERSIANN bias correction methods were chosen on both daily and monthly time scales, but EQM on a daily time scale and Delta on a monthly time scale were chosen for TMPA 3B42V7 satellite rainfall bias correction.

Table 5 | The general selected best bias correction and evaluation at both daily and monthly comparisons of Delta, EQM, and QM statistical methods corresponds with satellite rainfall products (CMORPH, TMPA_3B42V7, PERSIANN and CFSR) at five observed gauge stations of rainfall

		Overall selected BC methods	
Station	**SRPs**	**Daily**	**Monthly**
Pawe	CMORPH	Delta	Delta
	TMPA_3B42V7	Delta	Delta
	PERSIANN	Delta	Delta
	CFSR	Delta	Delta
Dangla	CMORPH	QM	Delta
	TMPA_3B42V7	EQM	EQM
	PERSIANN	EQM	EQM
	CFSR	Delta	Delta
Shahura	CMORPH	Delta	Delta
	TMPA_3B42V7	EQM	Delta
	PERSIANN	QM	QM
	CFSR	Delta	Delta
Durbete	CMORPH	QM	Delta
	TMPA_3B42V7	EQM	EQM
	PERSIANN	EQM	EQM
	CFSR	Delta	Delta
Yismala	CMORPH	Delta	Delta
	TMPA_3B42V7	EQM	Delta
	PERSIANN	EQM	EQM
	CFSR	Delta	Delta

4.2. Evaluation of raw data and satellite rainfall products

4.2.1. Daily comparison of satellite rainfall products

Table 6 shows the statistical indicators obtained for weather stations against the different satellite estimates (CMORPH, TMPA_3B42V7, and PERSIANN). In general, the result shows that the satellites are not very robust to estimate rainfall at the Main Beles basin. This is explained by the low values of the correlation coefficient ranging between 0.35 and 0.54. Relatively higher correlation coefficients (r) were obtained when CMORPH_QM (0.534) for the Dangla station, CMORPH_Delta &TMPA_3B42V7_Delta (0.45) for the Pawe station, TMPA_3B42V7_EQM (0.496) for the Shahura station, CMORPH_QM (0.538) for the Durbete station, and PERSIANN_EQM (0.442) for the Yismala station were correlated with data from the weather stations. The lowest correlation coefficient (0.348) was obtained when PERSIANN_EQM rainfall was correlated with the measured rainfall weather data at the Dangla weather station (Table 7 and Figure 5(a)). An index of agreement relatively close to one was scored by CMORPH_QM (0.716) more often than other products. This shows that there is a good index of agreement between the cumulative values of CMORPH_QM rainfall estimates and the cumulative value of each weather station. In addition, PERSIANN_EQM showed low MAE (average 3.489 mm day^{-1}) and RMSE (average 7.295 mm day^{-1}) were relatively close to zero for the Yismala station, whereas PERSIANN_EQM showed higher values (average 10.853 mm day^{-1}) deviating from zero for the Dangla station. To summarize for all stations based on the six statistical performances (RMSE, r, MAE, MBE, d, and NSE), CMORPH_Delta for the Pawe station, CMORPH_QM for Dangla and Shahura stations, TMPA_3B42V7_EQM for the Durbete station, and PERSIANN_EQM for the Yismala station are shown in Table 6 and Figure 5(a) and 5(b).

The Taylor diagram is shown for all gauging stations. In general, better correlation is shown for biased-corrected SRPs in comparison to uncorrected SRPs relative to *in situ* gauge stations. This is shown for all the gauging stations. Correlations vary from 0.348 to 0.538 for all gauge stations (Pawe, Dangla, Durbete, Shahura, and Yismala). The highest and lowest correlations were observed in CMORPH_QM (0.538) and PERSIANN_EQM (0.348) at stations Durbete and Dangla, respectively. At all stations, RMSE between gauge observations and bias-corrected SREs is between 7.457 and 10.853 mm day^{-1}. The maximum and the minimum RMSE values are 10.853 mm day^{-1} (PERSIANN_EQM) and 7.457 mm day^{-1} (CMORPH_Delta) for Dangla and Yismala weather stations, respectively (see Taylor's diagram for Figure 6). This shows that the lower value of RMSE is better relative to the higher value of bias-corrected SRPs. The lowest and highest value Standard Deviation (SD) were observed PERSIANN_EQM (7.23 mm/day) and TMPA_3B42V7_EQM (10.35 mm/day) at the Dangla and Shahura stations, respectively (Figure 6).

Table 6 | Summary of selected best bias correction and evaluation of daily comparison of Delta, EQM, and QM statistical methods corresponds with SRPs (CMORPH, TMPA_3B42V7, and PERSIANN) at five observed gauge stations of rainfall

Stations	SRPs	RMSE	r	MAE	MBE	d	NSE
Pawe	CMORPH_Delta	**9.237**	**0.450**	**4.397**	**0.000**	**0.647**	**0.025**
	TMPA_3B42V7_Delta	9.583	**0.450**	4.529	**0.000**	0.650	−0.049
	PERSIANN_Delta	10.128	0.361	4.878	**0.000**	0.579	−0.172
Dangla	CMORPH_QM	**8.590**	**0.534**	**4.474**	1.256	**0.711**	**0.004**
	TMPA_3B42V7_EQM	9.535	0.390	5.014	**0.238**	0.608	−0.227
	PERSIANN_EQM	10.853	0.348	5.246	0.431	0.567	−0.346
Shahura	CMORPH_Delta	**7.537**	0.471	**3.681**	**− 0.001**	0.662	**0.069**
	TMPA_3B42V7_EQM	8.264	**0.496**	4.110	1.022	**0.681**	− 0.119
	PERSIANN_QM	8.134	0.468	3.689	0.107	0.662	−0.084
Durbete	CMORPH_QM	8.392	**0.538**	4.346	0.912	**0.716**	0.032
	TMPA_3B42V7_EQM	**8.226**	0.530	**4.104**	**− 0.044**	0.714	**0.070**
	PERSIANN_EQM	9.115	0.401	4.602	−0.563	0.621	−0.142
Yismala	CMORPH_Delta	7.457	0.412	3.502	**0.000**	0.621	−0.175
	TMPA_3B42V7_EQM	7.813	0.406	4.029	0.790	0.619	−0.290
	PERSIANN_EQM	**7.295**	**0.442**	**3.489**	0.100	**0.647**	**− 0.125**

Bold numbers show the best-performing bias correction from the candidates.

Root mean square error (RMSE), correlation coefficient (r), mean absolute error (MAE), mean bias error (MBE), index of agreement (d), and Nash–Sutcliffe Efficiency (NSE) model are shown.

Table 7 | Comparison of SRPs (CMORPH, TMPA_3B42V7, and PERSIANN) with bias correction methods (Delta, EQM, and QM) related to five observed weather gauge stations of rainfall

Station	SRPs	RMSE	*r*	MAE	MBE	*d*	NSE
Pawe	CMORPH_Delta	2.47	**0.88**	**1.48**	**0.00**	**0.94**	**0.77**
	TMPA_3B42V7_Delta	**2.45**	**0.88**	1.51	−0.01	**0.94**	**0.77**
	PERSIANN_Delta	2.96	0.83	1.78	**0.00**	0.90	0.67
Dangla	CMORPH_Delta	1.92	**0.93**	1.20	**0.00**	**0.96**	0.85
	TMPA_3B42V7_EQM	**1.84**	**0.93**	1.24	0.24	**0.96**	**0.86**
	PERSIANN_EQM	2.37	0.88	1.52	0.04	0.94	0.77
Shahura	CMORPH_Delta	2.31	0.87	1.56	0.01	0.91	0.75
	TMPA_3B42V7_Delta	**1.70**	**0.93**	**1.14**	**0.00**	**0.96**	**0.86**
	PERSIANN_QM	2.15	0.89	1.26	0.10	0.94	0.78
Durbete	CMORPH_Delta	2.41	0.89	1.44	**0.00**	0.94	0.78
	TMPA_3B42V7_EQM	**1.59**	**0.95**	**1.10**	− 0.04	**0.97**	**0.90**
	PERSIANN_EQM	2.77	0.85	1.73	−0.56	0.91	0.71
Yismala	CMORPH_Delta	2.01	0.87	1.21	**0.00**	0.93	0.75
	TMPA_3B42V7_Delta	**1.77**	**0.90**	**1.08**	**0.00**	**0.95**	**0.81**
	PERSIANN_EQM	1.93	0.89	1.23	0.10	0.94	0.77

Bold numbers show the best-performing bias correction from the candidates.

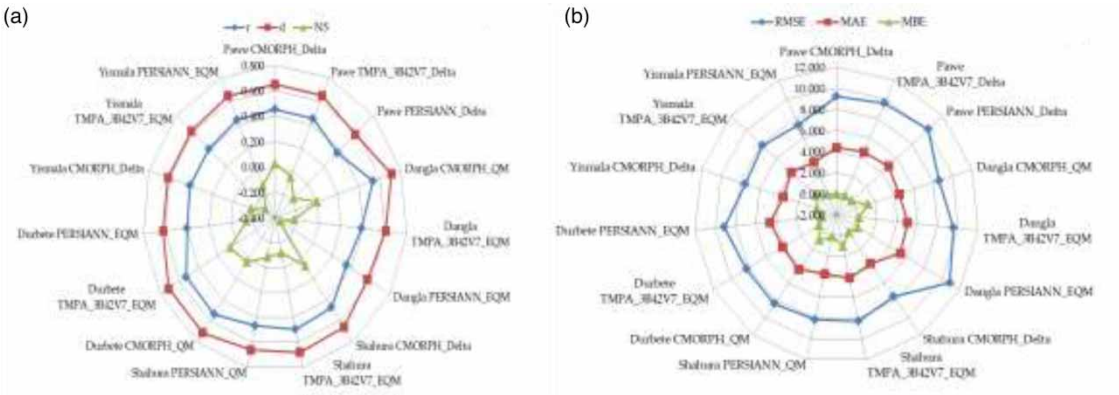

Figure 5 | The statistical indicators – correlation coefficient (*r*), index of agreement (*d*), and Nash–Sutcliffe Efficiency (NSE) model from (a) and RMSE, MAE, and MBE from (b) for each station at the daily time scale of SRPs (CMORPH, TMPA_3B42V7, and PERSIANN) with bias correction methods.

4.2.2. Monthly comparison satellite rainfall products

The monthly comparison of the satellite-derived rainfall with the weather stations was carried out using statistical approaches similar to those noted in section 4.2.1 for the daily time scale. The comparison was carried out using an independent rainfall dataset obtained from the five weather stations as shown in Figure 1. In general, good agreement between the three satellite-based rainfall estimates with the best bias correction methods and the weather station-based rainfall observations was found using Pearson's correlation coefficient (*r*) ranging from 0.83 to 0.95 (Table 7 and Figure 7(a)). TMPA_3B42V7_EQM scored the maximum ($r = 0.95$) at the Durbete station; the minimum was scored by PERSIANN_Delta ($r = 0.83$) at the Pawe station (Table 7 and Figure 7(a)). Overall, the six statistical performance evaluation criteria (RMSE, *r*, MAE, MBE, *d* and NSE) of SRPs corresponded with observed gauge stations very well for CMORPH_Delta, TMPA_3B42V7_EQM,TMPA_3B42V7_Delta,TMPA_3B42V7_EQM and TMPA_3B42V7_Delta related to the Pawe, Dangla, Shahura, Durbete and Yismala gauge stations, respectively, as shown in Table 7 and Figure 7(a) and (b).

The Taylor diagram is shown for all gauging stations (Figure 8). Correlations vary from 0.83 to 0.95 for all gauge stations (Pawe, Dangla, Durbete, Shahura, and Yismala) on a monthly time scale. PERSIANN_Delta for the lowest (0.83) and TMPA_3B42V7_EQM for the highest (0.95) correlation are observed for the Pawe and Durbete stations, respectively. At

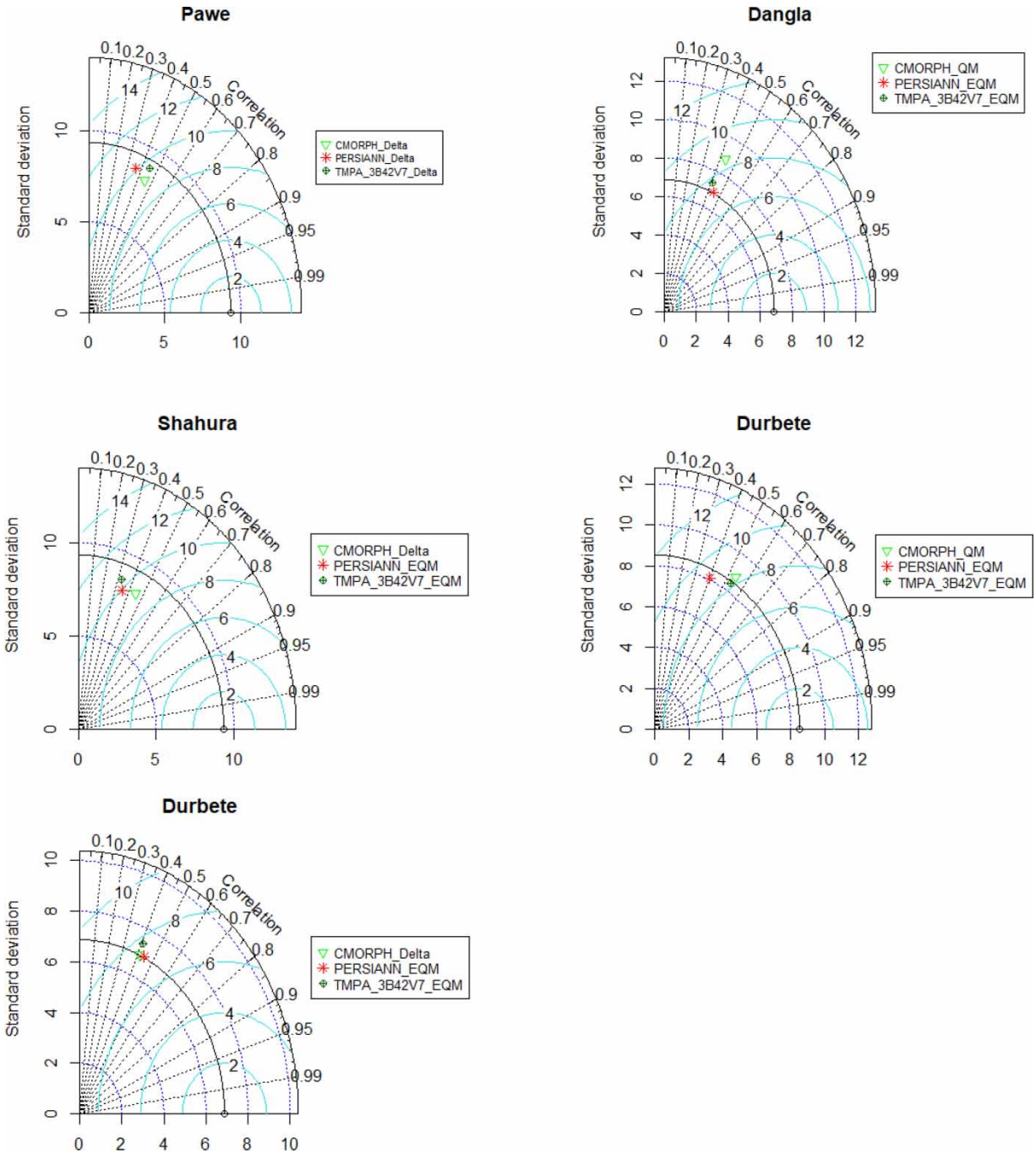

Figure 6 | Taylor's diagram for daily comparison of the temporal performances of multiple SRPs and multiple bias correction methods (Delta, EQM, and QM) against the ground-observed precipitation (the benchmark) for the baseline period (2003–2016). The azimuthal angle represents the correlation coefficient; radial distance represents the standard deviation (mm day^{-1}) of the rainfall time series and green contours represent RMSE (mm day^{-1}). Please refer to the online version of this paper to see this figure in colour: http://dx.doi.org/10.2166/wcc.2022.244.

all stations, RMSE relative to bias-corrected SREs and gauge observations are between 50.23 and 89.38 mm month^{-1}. The standard deviation (SD) of the lowest value for CMORPH_Delta (124.5 mm month^{-1}) and the highest value for CMORPH_QM (150.34 mm month^{-1}) are observed for Yismala and Dangla metrological stations, respectively (Figure 8).

In this study, the SRPs at two time scales (i.e., daily and monthly) were analyzed to identify satellite-derived rainfall data that could potentially be used for meteorological, hydrological, environmental, and drought-monitoring assessments in the

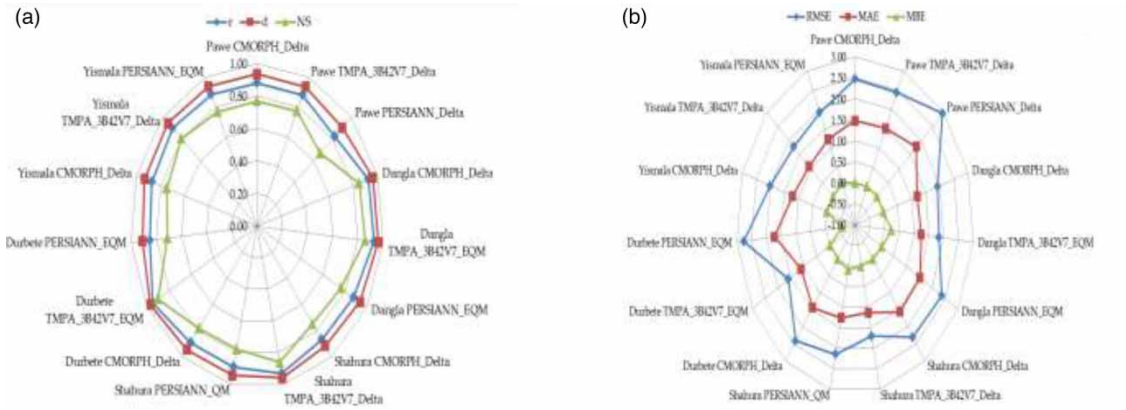

Figure 7 | The statistical indicators – (a) correlation coefficient (*r*), index of agreement (*d*), and Nash–Sutcliffe Efficiency (NSE) model and (b) RMSE, MAE, and MBE for each station at the monthly time scale of SRPs (CMORPH, TMPA_3B42V7, and PERSIANN) with bias correction methods.

Main Beles basin. Overall, the performance of the four rainfall-based satellite products (i.e., CFSR, CMORPH, TMPA_3B42V7, and PERSIANN) over the Main Beles basin is promising for further application in drought years. The result of comparative evaluation of these four satellite products and bias correction methods showed that CMORPH_Delta, CMORPH_QM, CMORPH_Delta, CMORPH_EQM, and CMORPH_EQM are the best satellite-derived rainfall data at daily scale, and CMORPH_Delta, TMPA_3B42V7_EQM, TMPA_3B42V7_Delta, TMPA_3B42V7_EQM, and TMPA_3B42V7_Delta are the best satellite-derived rainfall data at monthly time scales for Pawe, Dangla, Shahura, Durbete, and Yismala weather stations, respectively. Thus, this SRPs and bias correction methods were selected in this study for further application in the spatial and temporal assessment of meteorological and hydrological study in the Main Beles basin.

5. CONCLUSIONS

The availability of satellite-derived rainfall products at local and global scales has proved to be beneficial in filling the data gap, particularly in developing countries that have data scarcity. However, evaluating these rainfall products is essential for any application that includes studying water resource problems. In this regard, SRPs are a valuable source of information, particularly in sparsely gauged regions like the Main Beles watershed. In this study, we selected the three bias-corrected (Delta, EQM, and QM) methods and four SRPs (CMORPH, TMPA_3B42V7, PERSIANN, and CFSR) and evaluated the performances of three SRPs (CMORPH, TMPA_3B42V7, and PERSIANN) by comparing them with gauged rainfall data from five independent weather stations across the Main Beles basin for real-time hydrological applications. The statistical approach was used for the performance evaluation at daily and monthly time scales. The evaluation process was undertaken to identify the best SRP and bias correction methods for the spatial and temporal assessment of meteorological data in the basin. After analyzing the results, the following conclusions were drawn.

In general, the bias correction achieved significantly improved the ability of these products to hydrology forecast on a daily and monthly scale. This result is in agreement with previous findings that have suggested that rainfall correction methods have a more significant influence than temperature correction methods. Delta performed better than QM and EQM for the Pawe station for five SRPs at both daily and monthly time scales only when the estimates in the datasets were highly cross-correlated. For the Dangla station, EQM was selected for TMPA_3B42V7 and PERSIANN bias correction on both daily and monthly time scales, but Delta was selected for CFSR bias correction on both daily and monthly time scales and QM at daily and Delta at monthly bias correction method selected for CMORPH SRPs. For the Shahura station, Delta for CMORPH and CFSR and also QM for PERSIANN bias correction methods were selected for both daily and monthly time scales, but EQM at daily and Delta at monthly time scales selected for TMPA_3B42V7 satellite rainfall bias correction. For the Durbete station, EQM for TMPA_3B42V7 and PERSIANN and also Delta for CFSR bias correction methods were selected for both daily and monthly time scales but QM at daily and Delta at monthly for CMORPH satellite rainfall bias correction were selected. For the Yismala station, Delta for CMORPH and CFSR and also EQM for PERSIANN bias correction methods were selected for both daily and monthly time scales, but EQM at daily and Delta at monthly time scales were

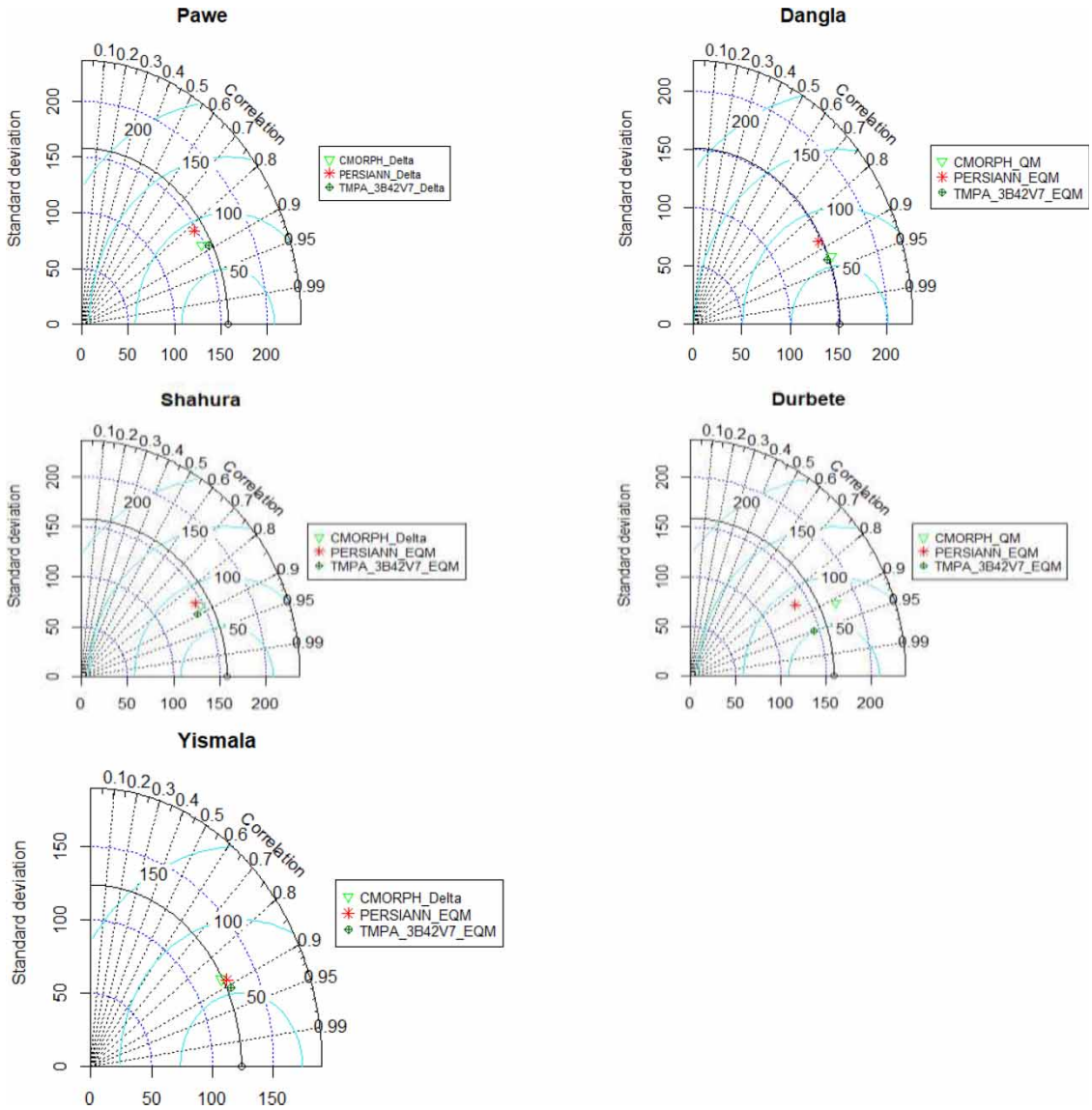

Figure 8 | Taylor's diagram for daily comparing the temporal performances of multiple SRPs and multiple bias correction methods (Delta, EQM, and QM) against the ground-observed precipitation (the benchmark) for the baseline period (2003–2016). The azimuthal angle represents correlation coefficient; radial distance represents the standard deviation (mm day^{-1}) of the rainfall time series and green contours represent RMSE (mm day^{-1}). Please refer to the online version of this paper to see this figure in colour: http://dx.doi.org/10.2166/wcc.2022.244.

selected for TMPA_3B42V7 satellite rainfall bias correction. Both the bias correction methods (EQM, QM, and Delta) improved the quality of SRPs, and consequently, they have a direct influence over the accuracy of hydrological simulations.

The performance of the three SRPs (TMPA_3B42V7, PERSIANN, and CMORPH) was reasonably good in detecting the occurrence of rainfall and in estimating the amount of daily and monthly rainfall in the basin. Comparison of the three SRPs has shown that good agreement ($r > 0.4$) of CMORPH_ Delta, CMORPH_QM, CMORPH_Delta, CMORPH_EQM, and CMORPH_EQM at daily time scale and at the monthly time scale of agreement ($r > 0.88$) of CMORPH_Delta, TMPA_3B42V7_EQM, TMPA_3B42V7_Delta, TMPA_3B42V7_EQM, and TMPA_3B42V7_Delta rainfall products and bias correction methods with ground observations of Pawe, Dangla, Shahura, Durbete and Yismala weather stations, respectively, and the overall statistical weighting performances (i.e., Pearson's correlation coefficient (r), MAE, MBE, RMSE, index of agreement (d), and Nash–Sutcliffe Efficiency (NSE) model) are also good. The results depicted that SRPs and bias correction methods of CMORPH_QM ($r = 0.538$) and TMPA_3B42V7_EQM ($r = 0.95$) data showed good performance, while PERSIANN_EQM ($r = 0.348$) and PERSIANN_Delta ($r = 0.83$) perform worst at daily and monthly time scales, respectively,

among the others. This shows that both SRPs and bias correction methods can be used to develop operational drought or flood monitoring, any hydrological study, and early warning system since daily and monthly time scales better identify periods of low or heavy rainfall events in the study area with each metrological station.

Improvements in hydrological forecasts obtained by bias-correcting raw rainfall estimates can help to enhance the operation of reservoirs, planning for irrigation, and construction of hydraulic works, among other things. This process is undoubtedly relevant for forecasting future scenarios in which the pressure exerted by users of water resources increases. Additionally, it is worth mentioning that since these bias correction methods are assumed to be stationary, the correction algorithm and its parameterization can be valid for current climate conditions. However, further research is necessary on this topic to clearly determine the ability of these bias correction methods to correct future raw estimates in the Main Beles basin under different climate scenarios.

ACKNOWLEDGEMENTS

The authors would like to extend their gratitude to the Amhara National Metrological Agency (NMA) of Ethiopia for the provision of valuable data for this research. The authors also thankful the reviewers for their thoughtful comments. A.B.N. would like to thank the facilities provided by the Wollo University/Kombolcha Institute of Technology (KIoT) and friends for their appreciative support for doing this research. A.B.N. is also thankful to IWA Publishing for Subscribe to Open (S2O) platform and for supporting developing countries.

AUTHOR CONTRIBUTIONS

A.B.N. and H.W.T. conceptualized the whole article. A.B.N., F.A., and H.W.T. developed the methodology. A.B.N. was involved in data curation and wrote the original draft. H.W.T., A.E., F.A., and G.W. wrote the original draft and the review, and edited the article. A.E. and G.W. supervised the work. All authors have read and agreed to the published version of the manuscript.

FUNDING

The authors did not receive support from any organization for the submitted work.

DATA AVAILABILITY STATEMENT

The data used in this study are available from the authors on reasonable request and some data obtained from: CMORPH (https://climatedataguide.ucar.edu/), TMPA_3B42V7 (https://mirador.gsfc.nasa.gov/), PERSIANN (https://chrsdata.eng.uci.edu/), and CFSR (https://globalweather.tamu.edu/).

CONFLICT OF INTEREST

The authors declare there is no conflict.

REFERENCES

Annys, S., Adgo, E., Ghebreyohannes, T., Van Passel, S., Dessein, J. & Nyssen, J. 2019 Impacts of the hydropower-controlled Tana-Beles interbasin water transfer on downstream rural livelihoods (northwest Ethiopia). *Journal of Hydrology* **569**, 436–448.

Ayoub, A. B., Tangang, F., Juneng, L., Tan, M. L. & Chung, J. X. 2020 Evaluation of gridded precipitation datasets in Malaysia. *Remote Sensing* **12** (4), 613.

Bao, X. & Zhang, F. 2013 Evaluation of NCEP–CFSR, NCEP–NCAR, ERA-Interim, and ERA-40 reanalysis datasets against independent sounding observations over the Tibetan Plateau. *Journal of Climate* **26** (1), 206–214.

Belay, A. S., Fenta, A. A., Yenehun, A., Nigate, F., Tilahun, S. A., Moges, M. M., Dessie, M., Adgo, E., Nyssen, J. & Chen, M. 2019 Evaluation and application of multi-source satellite rainfall product CHIRPS to assess spatio-temporal rainfall variability on data-sparse western margins of Ethiopian highlands. *Remote Sensing* **11** (22), 2688.

Bhatti, H. A., Rientjes, T., Haile, A. T., Habib, E. & Verhoef, W. 2016 Evaluation of bias correction method for satellite-based rainfall data. 1–16. https://doi.org/10.3390/s16060884.

Boé, J., Terray, L., Habets, F. & Martin, E. 2007 Statistical and dynamical downscaling of the Seine basin climate for hydro-meteorological studies. *International Journal of Climatology* **27** (12), 1643–1655.

Centella-Artola, A., Bezanilla-Morlot, A., Taylor, M. A., Herrera, D. A., Martinez-Castro, D., Gouirand, I., Sierra-Lorenzo, M., Vichot-Llano, A., Stephenson, T. & Fonseca, C. 2020 Evaluation of sixteen gridded precipitation datasets over the Caribbean region using gauge observations. *Atmosphere* **11** (12), 1334.

Collischonn, B., Collischonn, W. & Tucci, C. E. M. 2008 Daily hydrological modeling in the Amazon basin using TRMM rainfall estimates. *Journal of Hydrology* **360** (1–4), 207–216.

Conti, F. L., Hsu, K.-L., Noto, L. V. & Sorooshian, S. 2014 Evaluation and comparison of satellite precipitation estimates with reference to a local area in the Mediterranean Sea. *Atmospheric Research* **138**, 189–204.

Dembélé, M. & Zwart, S. J. 2016 Evaluation and comparison of satellite-based rainfall products in Burkina Faso, West Africa. *International Journal of Remote Sensing* **37** (17), 3995–4014.

Derin, Y. & Yilmaz, K. K. 2014 Evaluation of multiple satellite-based precipitation products over complex topography. *Journal of Hydrometeorology* **15** (4), 1498–1516.

Dile, Y. T. & Srinivasan, R. 2014 Evaluation of CFSR climate data for hydrologic prediction in data-scarce watersheds: an application in the Blue Nile River Basin. *JAWRA Journal of the American Water Resources Association* **50** (5), 1226–1241.

Dinku, T., Ceccato, P., Grover-Kopec, E., Lemma, M., Connor, S. J. & Ropelewski, C. F. 2007 Validation of satellite rainfall products over East Africa's complex topography. *International Journal of Remote Sensing* **28** (7), 1503–1526.

Ebrahim, G. Y., Jonoski, A., Van Griensven, A. & Di Baldassarre, G. 2013 Downscaling technique uncertainty in assessing hydrological impact of climate change in the Upper Beles River Basin, Ethiopia. *Hydrology Research* **44** (2), 377–398.

Enayati, M., Bozorg-Haddad, O., Bazrafshan, J., Hejabi, S. & Chu, X. 2021 Bias correction capabilities of quantile mapping methods for rainfall and temperature variables. *Journal of Water and Climate Change* **12** (2), 401–419.

Ferraro, R. R. 1997 Special sensor microwave imager derived global rainfall estimates for climatological applications. *Journal of Geophysical Research: Atmospheres* **102** (D14), 16715–16735.

Ferraro, R. R., Weng, F., Grody, N. C. & Zhao, L. 2000 Precipitation characteristics over land from the NOAA-15 AMSU sensor. *Geophysical Research Letters* **27** (17), 2669–2672.

Funk, C., Peterson, P., Landsfeld, M., Pedreros, D., Verdin, J., Shukla, S., Husak, G., Rowland, J., Harrison, L. & Hoell, A. 2015 The climate hazards infrared precipitation with stations – a new environmental record for monitoring extremes. *Scientific Data* **2** (1), 1–21.

Habib, E., Haile, A. T., Sazib, N., Zhang, Y. & Rientjes, T. 2014 *Effect of Bias Correction of Satellite-Rainfall Estimates on Runoff Simulations at the Source of the Upper Blue Nile*, pp. 6688–6708. https://doi.org/10.3390/rs6076688.

Haile, A. T., Habib, E. & Rientjes, T. 2013 Evaluation of the climate prediction center (CPC) morphing technique (CMORPH) rainfall product on hourly time scales over the source of the Blue Nile River. *Hydrological Processes* **27** (12), 1829–1839.

Hall, J., Arheimer, B., Borga, M., Brázdil, R., Claps, P., Kiss, A., Kjeldsen, T. R., Kriauciuniene, J., Kundzewicz, Z. W. & Lang, M. 2014 *Understanding Flood Regime Changes in Europe: A State of the art Assessment*.

Hamlet, A. F. & Lettenmaier, D. P. 1999 Effects of climate change on hydrology and water resources in the Columbia River Basin 1. *JAWRA Journal of the American Water Resources Association* **35** (6), 1597–1623.

Hamza, A. A. & Getahun, B. A. 2022 Assessment of water resource and forecasting water demand using WEAP model in Beles river, Abbay river basin, Ethiopia. *Sustainable Water Resources Management* **8** (1), 1–14.

Hsu, K., Gao, X., Sorooshian, S. & Gupta, H. V. 1997 Precipitation estimation from remotely sensed information using artificial neural networks. *Journal of Applied Meteorology* **36** (9), 1176–1190.

Huffman, G. J., Bolvin, D. T., Nelkin, E. J., Wolff, D. B., Adler, R. F., Gu, G., Hong, Y., Bowman, K. P. & Stocker, E. F. 2007 The TRMM multisatellite precipitation analysis (TMPA): quasi-global, multiyear, combined-sensor precipitation estimates at fine scales. *Journal of Hydrometeorology* **8** (1), 38–55.

Joyce, R. J., Janowiak, J. E., Arkin, P. A. & Xie, P. 2004 CMORPH: a method that produces global precipitation estimates from passive microwave and infrared data at high spatial and temporal resolution. *Journal of Hydrometeorology* **5** (3), 487–503.

Kebede, Y. S., Endalamaw, N. T., Sinshaw, B. G. & Atinkut, H. B. 2021 Modeling soil erosion using RUSLE and GIS at watershed level in the upper Beles, Ethiopia. *Environmental Challenges* **2**, 100009.

Kummerow, C., Hong, Y., Olson, W. S., Yang, S., Adler, R. F., McCollum, J., Ferraro, R., Petty, G., Shin, D.-B. & Wilheit, T. T. 2001 The evolution of the Goddard Profiling Algorithm (GPROF) for rainfall estimation from passive microwave sensors. *Journal of Applied Meteorology* **40** (11), 1801–1820.

Lemann, T., Roth, V., Zeleke, G., Subhatu, A., Kassawmar, T. & Hurni, H. 2018 Spatial and temporal variability in hydrological responses of the Upper Blue Nile basin, Ethiopia. *Water* **11** (1), 21.

Liu, J., Shanguan, D., Liu, S. & Ding, Y. 2018 Evaluation and hydrological simulation of CMADS and CFSR reanalysis datasets in the Qinghai-Tibet Plateau. *Water* **10** (4), 513.

Liu, Y., Weerts, A. H., Clark, M., Hendricks Franssen, H.-J., Kumar, S., Moradkhani, H., Seo, D.-J., Schwanenberg, D., Smith, P. & Van Dijk, A. 2012 Advancing data assimilation in operational hydrologic forecasting: progresses, challenges, and emerging opportunities. *Hydrology and Earth System Sciences* **16** (10), 3863–3887.

López López, P., Immerzeel, W. W., Rodríguez Sandoval, E. A., Sterk, G. & Schellekens, J. 2018 Spatial downscaling of satellite-based precipitation and its impact on discharge simulations in the Magdalena River basin in Colombia. *Frontiers in Earth Science* **6**, 68.

Luo, M., Liu, T., Meng, F., Duan, Y., Frankl, A., Bao, A. & De Maeyer, P. 2018 Comparing bias correction methods used in downscaling precipitation and temperature from regional climate models: a case study from the Kaidu River Basin in Western China. *Water* **10** (8), 1046.

Martinez-Villalobos, C. & Neelin, J. D. 2019 Why do precipitation intensities tend to follow gamma distributions? *Journal of the Atmospheric Sciences* **76** (11), 3611–3631.

Moges, D. M., Kmoch, A. & Uuemaa, E. 2022 Application of satellite and reanalysis precipitation products for hydrological modeling in the data-scarce Porijõgi catchment, Estonia. *Journal of Hydrology: Regional Studies* **41**, 101070.

Molla, G. A., Desta, G. & Dananto, M. 2022 Soil management and crop practice effect on soil water infiltration and soil water storage in the humid lowlands of Beles Sub-Basin, Ethiopia. *Hydrology* **10**, 1–11.

Nguyen, P., Ombadi, M., Sorooshian, S., Hsu, K., AghaKouchak, A., Braithwaite, D., Ashouri, H. & Thorstensen, A. R. 2018 The PERSIANN family of global satellite precipitation data: a review and evaluation of products. *Hydrology and Earth System Sciences* **22** (11), 5801–5816.

Nguyen, P., Shearer, E. J., Tran, H., Ombadi, M., Hayatbini, N., Palacios, T., Huynh, P., Braithwaite, D., Updegraff, G. & Hsu, K. 2019 The CHRS data portal, an easily accessible public repository for PERSIANN global satellite precipitation data. *Scientific Data* **6** (1), 1–10.

Oruc, S. 2022 Performance of bias corrected monthly CMIP6 climate projections with different reference period data in Turkey. *Acta Geophysica* **70** (2), 777–789.

Prakash, S., Mitra, A. K., Momin, I. M., Pai, D. S., Rajagopal, E. N. & Basu, S. 2015 Comparison of TMPA-3B42 versions 6 and 7 precipitation products with gauge-based data over India for the southwest monsoon period. *Journal of Hydrometeorology* **16** (1), 346–362.

Prakash, S., Mitra, A. K., Rajagopal, E. N. & Pai, D. S. 2016 Assessment of TRMM-based TMPA-3b42 and GSMaP precipitation products over India for the peak southwest monsoon season. *International Journal of Climatology* **36** (4), 1614–1631.

Revilla-Romero, B., Hirpa, F. A., Thielen-del Pozo, J., Salamon, P., Brakenridge, R., Pappenberger, F. & De Groeve, T. 2015 On the use of global flood forecasts and satellite-derived inundation maps for flood monitoring in data-sparse regions. *Remote Sensing* **7** (11), 15702–15728.

Ringard, J., Seyler, F. & Linguet, L. 2017 A quantile mapping bias correction method based on hydroclimatic classification of the Guiana shield. *Sensors* **17** (6), 1413.

Sharp, E., Dodds, P., Barrett, M. & Spataru, C. 2015 Evaluating the accuracy of CFSR reanalysis hourly wind speed forecasts for the UK, using in situ measurements and geographical information. *Renewable Energy* **77**, 527–538.

Smiatek, G., Kunstmann, H. & Senatore, A. 2016 EURO-CORDEX regional climate model analysis for the Greater Alpine Region: performance and expected future change. *Journal of Geophysical Research: Atmospheres* **121** (13), 7710–7728.

Sorooshian, S., Nguyen, P., Sellars, S., Braithwaite, D., AghaKouchak, A. & Hsu, K. 2014 Satellite-based remote sensing estimation of precipitation for early warning systems. *Extreme Natural Hazards, Disaster Risks and Societal Implications* **1**, 99.

Srivastava, P. K., Islam, T. & Gupta, M. 2015 WRF dynamical downscaling and bias correction schemes for NCEP estimated hydro-meteorological variables. https://doi.org/10.1007/s11269-015-0940-z.

Taylor, K. E. 2001 Summarizing multiple aspects of model performance in a single diagram. *Journal of Geophysical Research: Atmospheres* **106** (D7), 7183–7192.

Thiemig, V., Rojas, R., Zambrano-Bigiarini, M., Levizzani, V. & De Roo, A. 2012 Validation of satellite-based precipitation products over sparsely gauged African river basins. *Journal of Hydrometeorology* **13** (6), 1760–1783.

Vu, T. T., Li, L. & Jun, K. S. 2018 Evaluation of multi-satellite precipitation products for streamflow simulations: a case study for the Han River Basin in the Korean Peninsula, East Asia. *Water* **10** (5), 642.

WaleWorqlul, A., Taddele, Y. D., Ayana, E. K., Jeong, J., Adem, A. A. & Gerik, T. 2018 Impact of climate change on streamflow hydrology in headwater catchments of the upper Blue Nile Basin, Ethiopia. *Water (Switzerland)* **10** (2). https://doi.org/10.3390/w10020120.

Wei, S.-W., Lu, C.-H., Liu, Q., Collard, A., Zhu, T., Grogan, D., Li, X., Wang, J., Grumbine, R. & Bhattacharjee, P. S. 2021 The impact of aerosols on satellite radiance data assimilation using NCEP global data assimilation system. *Atmosphere* **12** (4), 432.

Woldesenbet, T. A., Elagib, N. A., Ribbe, L. & Heinrich, J. 2017 Hydrological responses to land use/cover changes in the source region of the Upper Blue Nile Basin, Ethiopia. *Science of the Total Environment* **575**, 724–741.

Yang, W.-T., Fu, S.-M., Sun, J.-H., Zheng, F., Wei, J. & Ma, Z. 2021 Comparative evaluation of the performances of TRMM-3b42 and Climate Prediction Centre Morphing Technique (CMORPH) precipitation estimates over Thailand. *Journal of the Meteorological Society of Japan Ser. II* **99** (6), 1525–1546.

Yasir, S. A., Crosato, A., Mohamed, Y. A., Abdalla, S. H. & Wright, N. G. 2014 Sediment balances in the Blue Nile River basin. *International Journal of Sediment Research* **29** (3), 316–328.

Yimer, G., Jonoski, A. & Griensven, A. V. 2009 Hydrological response of a catchment to climate change in the upper Beles river basin, upper blue Nile, Ethiopia. *Nile Basin Water Engineering Scientific Magazine* **2** (1), 49–59.

Yong, B., Chen, B., Gourley, J. J., Ren, L., Hong, Y., Chen, X., Wang, W., Chen, S. & Gong, L. 2014 Intercomparison of the Version-6 and Version-7 TMPA precipitation products over high and low latitudes basins with independent gauge networks: is the newer version better in both real-time and post-real-time analysis for water resources and hydrologic ext. *Journal of Hydrology* **508**, 77–87.

Zambrano-Bigiarini, M., Nauditt, A., Birkel, C., Verbist, K. & Ribbe, L. 2017 Temporal and spatial evaluation of satellite-based rainfall estimates across the complex topographical and climatic gradients of Chile. *Hydrology and Earth System Sciences* **21** (2), 1295.

First received 24 June 2022; accepted in revised form 3 December 2022. Available online 15 December 2022